

Spectrum of cosmic-ray nucleons, kaon production, and the atmospheric muon charge ratio

Thomas K. Gaisser

*Bartol Research Institute and Dept. of Physics and Astronomy
University of Delaware, Newark, DE, USA*

Abstract

Interpretation of measurements of the muon charge ratio in the TeV range depends on the spectra of protons and neutrons in the primary cosmic radiation and on the inclusive cross sections for production of π^\pm and K^\pm in the atmosphere. Recent measurements of the spectra of cosmic-ray nuclei are used here to estimate separately the energy spectra of protons and neutrons and hence to calculate the charge separated hadronic cascade in the atmosphere. From the corresponding production spectra of μ^+ and μ^- the μ^+/μ^- ratio is calculated and compared to recent measurements. The comparison leads to a determination of the relative contribution of kaons and pions. Implications for the spectra of ν_μ and $\bar{\nu}_\mu$ are discussed.

1. Introduction

The muon charge ratio in the TeV range has been measured by MINOS [1, 2] and more recently by OPERA [3]. Both analyses use an analytic approximation as a framework for making an inference about the separate contributions of the pion and kaon channels to the charge asymmetry. In this paper a more detailed derivation of the muon charge ratio is used for the analysis. The muon charge ratio is expressed in terms of the spectrum-weighted moments for production of π^\pm and K^\pm by protons and neutrons in the primary cosmic radiation, following the analysis of Lipari [4]. The analysis here accounts for the special contribution of associated production of charged, positive kaons.

Email address: gaisser@bartol.udel.edu (Thomas K. Gaisser)

This analysis also accounts for the effect of the energy dependence of the composition of the primary cosmic-ray nuclei. Measurements from ATIC [5] and CREAM [6, 7] indicate that the spectra of helium and heavier nuclei become somewhat harder than the spectrum of protons above several hundred GeV. This feature for helium was recently confirmed by PAMELA [8].

Because muon neutrinos are produced together with muons in the processes

$$\pi^\pm \rightarrow \mu^\pm + \nu_\mu(\bar{\nu}_\mu) \text{ and } K^\pm \rightarrow \mu^\pm + \nu_\mu(\bar{\nu}_\mu), \quad (1)$$

these results also apply to ν_μ and $\bar{\nu}_\mu$. In the TeV range and above the contribution of muon decay to the intensity of muon neutrinos is negligible. For reasons of kinematics, kaons are relatively more important for neutrinos at high energy than for muons. An additional goal of this paper is to draw attention to the implications of the muon results for atmospheric neutrinos in the TeV energy range and beyond.

2. Muon charge ratio

The excess of μ^+ in atmospheric muons can be traced to the excess of protons over neutrons in the primary cosmic-ray beam coupled with the steepness of the cosmic-ray spectrum, which emphasizes the forward fragmentation region in interactions of the incident cosmic-ray nucleons. The classic derivation of the muon charge ratio [9] considers muon production primarily through the channel $p \rightarrow \pi^\pm + \text{anything}$. The atmospheric cascade equation for the intensity of nucleons as a function of slant depth X in the atmosphere is solved separately for $N = n + p$ and $\Delta = p - n$ subject to the appropriate boundary conditions. For the total intensity of nucleons as a function of slant depth X (g/cm^2)

$$\phi_N(E) = \phi_N(0) \times \exp\left(-\frac{X}{\Lambda_N}\right) \quad (2)$$

where the nucleon attenuation length is $\Lambda_N = \lambda/(1 - Z_{NN})$ and λ is the interaction length of nucleons in the atmosphere. The corresponding result for $\Delta(X) = p(X) - n(X)$ is

$$\Delta(X) = \delta_0 \phi_N(0) \times \exp\left(-\frac{X}{\Lambda_-}\right), \quad (3)$$

where

$$\delta_0 = \frac{p(0) - n(0)}{p(0) + n(0)} \text{ and } \frac{1}{\Lambda_-} = \frac{1 - Z_{pp} + Z_{pn}}{1 + Z_{pp} + Z_{pn}} \frac{1}{\Lambda_N}. \quad (4)$$

The Z -factors (like $Z_{NN} = Z_{pp} + Z_{pn}$) are spectrum-weighted moments of the inclusive cross sections for the corresponding hadronic process. For example, a particularly important moment for this paper is

$$Z_{pK^+} = \frac{1}{\sigma} \int x^\gamma \frac{d\sigma(x)}{dx} dx \quad (5)$$

for the process

$$p + air \rightarrow K^+ + \Lambda + \text{anything}. \quad (6)$$

The normalized inclusive cross section is weighted by x^γ where γ is the integral spectral index for a power-law spectrum and $x = E_K/E_p$. Feynman scaling is assumed in these approximate formulas, so the parameters may vary slowly with energy, especially near threshold. However, the scaling approximation is relatively good because the moment weights the forward fragmentation region.

2.1. Charged pion channel

The next step is to solve the coupled equations for the production of charged pions by nucleons separately for $\Pi^+(X) + \Pi^-(X)$ and for $\Delta_\pi = \Pi^+(X) - \Pi^-(X)$. The solutions are then convolved with the probability per g/cm² for decay to obtain the corresponding production spectra of muons and neutrinos. The decay kinematic factors are

$$\frac{1 - r_\pi^{\gamma+1}}{(\gamma + 1)(1 - r_\pi)} \quad \text{and} \quad \frac{\epsilon_\pi}{\cos \theta E_\mu} \frac{1 - r_\pi^{\gamma+2}}{(\gamma + 2)(1 - r_\pi)} \quad (7)$$

for muons and

$$\frac{(1 - r_\pi)^\gamma}{(\gamma + 1)} \quad \text{and} \quad \frac{\epsilon_\pi}{\cos \theta E_\mu} \frac{(1 - r_\pi)^{(\gamma+1)}}{(\gamma + 2)} \quad (8)$$

for neutrinos. In each of Eqs. 7 and 8 the first expression is a low-energy limit and the second a high energy limit, where low and high are with respect to the critical energy ϵ_π . The ratio $r_\pi = m_\mu^2/m_\pi^2 = 0.5731$. The forms for two-body decay of charged kaons are the same with $r_K = 0.0458$.

The production spectra are then integrated over slant depth through the atmosphere to obtain the corresponding contributions to the lepton fluxes. Finally, the low and high-energy forms are combined into a single approximate expression.

For example, for the flux of $\nu_\mu + \bar{\nu}_\mu$ the expression is

$$\begin{aligned} \phi_\nu(E_\nu) &= \phi_N(E_\nu) \\ &\times \left\{ \frac{A_{\pi\nu}}{1 + B_{\pi\nu} \cos(\theta) E_\nu / \epsilon_\pi} + \frac{A_{K\nu}}{1 + B_{K\nu} \cos(\theta) E_\nu / \epsilon_K} \right. \\ &\quad \left. + \frac{A_{\text{charm}\nu}}{1 + B_{\text{charm}\nu} \cos(\theta) E_\nu / \epsilon_{\text{charm}}} \right\}. \end{aligned} \quad (9)$$

Here $\phi_N(E_\nu) = dN/d\ln(E_\nu)$ is the primary spectrum of nucleons (N) evaluated at the energy of the neutrino. The three terms in brackets correspond to production from leptonic and semi-leptonic decays of pions, kaons and charmed hadrons respectively. The term for prompt neutrinos from decay of charm has been included in Eq. 9 (see Ref. [10]) but will not be discussed further here.

The numerator of each term of Eq. 9 has the form

$$A_{i\nu} = \frac{Z_{Ni} \times BR_{i\nu} \times Z_{i\nu}}{1 - Z_{NN}} \quad (10)$$

with $i = \pi^\pm, K$, charm and $BR_{i\nu}$ is the branching ratio for $i \rightarrow \nu$. The first Z -factor in the numerator is the spectrum weighted moment of the cross section for a nucleon (N) to produce a secondary hadron i from a target nucleus in the atmosphere, defined as in Eq. 5. The second Z -factor is the corresponding moment of the decay distribution for $i \rightarrow \nu + X$, which is written explicitly in Eq. 8. The second term in each denominator is the ratio of the low-energy to the high-energy form of the decay distribution [11]. The forms for muons are the same, but the kinematic factors differ in a significant way (Eq. 7 instead of Eq. 8). Explicitly, for neutrinos

$$B_{\pi\nu} = \left(\frac{\gamma + 2}{\gamma + 1} \right) \left(\frac{1}{1 - r_\pi} \right) \left(\frac{\Lambda_\pi - \Lambda_N}{\Lambda_\pi \ln(\Lambda_\pi / \Lambda_N)} \right) \quad (11)$$

and for muons

$$B_{\pi\mu} = \left(\frac{\gamma + 2}{\gamma + 1} \right) \left(\frac{1 - (r_\pi)^{\gamma+1}}{1 - (r_\pi)^{\gamma+2}} \right) \left(\frac{\Lambda_\pi - \Lambda_N}{\Lambda_\pi \ln(\Lambda_\pi / \Lambda_N)} \right). \quad (12)$$

The forms for kaons are the same as functions of r_K and Λ_K .

The separate solutions for $\pi^+ \rightarrow \mu^+ + \nu_\mu$ and $\pi^- \rightarrow \mu^- + \bar{\nu}_\mu$ have the form

$$\phi_\pi(E_\mu)^\pm = \phi_N(E_\mu) \frac{A_{\pi\mu} \times 0.5(1 \pm \alpha_\pi \beta \delta_0)}{1 + B_{\pi\mu}^\pm \cos(\theta) E_\mu / \epsilon_\pi}, \quad (13)$$

where

$$B_{\pi\mu}^{\pm} = B_{\pi\mu} \frac{1 \pm \alpha_{\pi}\beta\delta_0}{1 \pm c_{\pi}\alpha_{\pi}\beta\delta_0}.$$

Here

$$\beta = \frac{1 - Z_{pp} - Z_{pn}}{1 - Z_{pp} + Z_{pn}} \approx 0.909; \quad \beta_{\pi} = \frac{1 - Z_{\pi^+\pi^+} - Z_{\pi^+\pi^-}}{1 - Z_{\pi^+\pi^+} + Z_{\pi^+\pi^-}} \approx 0.929;$$

$$\alpha_{\pi} = \frac{Z_{p\pi^+} - Z_{p\pi^-}}{Z_{p\pi^+} + Z_{p\pi^-}} \approx 0.165$$

and

$$c_{\pi} = \frac{1 - \Lambda_N/\Lambda_{\pi}}{1 - \beta\Lambda_N/(\beta_{\pi}\Lambda_{\pi})} \left[1 + \frac{\ln(\beta_{\pi}/\beta)}{\ln(\Lambda_{\pi}/\Lambda_N)} \right] \approx 1.01.$$

The numerical values are based on fixed target data in the energy range of hundreds of GeV [11]. The factors $B_{\pi\mu}^{\pm}$ differ by less than one per cent. To this accuracy, the charge ratio of muons can therefore be written in the form

$$\frac{\mu^+}{\mu^-} \approx \frac{1 + \beta\delta_0\alpha_{\pi}}{1 - \beta\delta_0\alpha_{\pi}} = \frac{f_{\pi^+}}{1 - f_{\pi^+}}, \quad (14)$$

where $f_{\pi^+} = (1 + \beta\delta_0\alpha_{\pi})/2$ is the fraction of positive muons from decay of charged pions.

2.2. Leptons from decay of kaons

The situation becomes more complex when the contribution from kaons is considered. In the first place, because the critical energies are significantly different for pions and kaons, the two contributions have to be followed separately. In addition the charge ratio of muons from decay of charged kaons is larger than that from pion decay because the process of associated production in Eq. 6 has no analog for forward production of K^- . Instead, associated production by neutrons leads to $\Lambda \bar{K}^0$.

For the charge separated analysis of kaons it is useful to divide kaon production by nucleons into a part in which K^+ and K^- are produced equally by neutrons and by protons and another for associated production, which is treated separately. Then in the approximation that kaon production by pions in the cascade is neglected, the spectrum of negative muons from decay of K^- is

$$\phi_K(E_{\mu})^- = \frac{Z_{NK^-}}{Z_{NK}} \phi_N(E_{\mu}) \frac{A_{NK}}{1 + B_{K\mu} \cos(\theta) E_{\mu}/\epsilon_K}. \quad (15)$$

There is an equal contribution of central production to positive kaons, but in addition there is the contribution from associated production. The total contribution of the kaon channel to positive muons is

$$\phi_K(E_\mu)^+ = \phi_N(E_\mu) A_{NK} \times \frac{\frac{1}{2}(1 + \alpha_K \beta \delta_0)}{1 + B_{K\mu}^+ \cos(\theta) E_\mu / \epsilon_K}. \quad (16)$$

Here

$$\alpha_K = \frac{Z_{pK^+} - Z_{pK^-}}{Z_{pK^+} + Z_{pK^-}}$$

and

$$B_{K\mu}^+ = B_{K\mu} \times \frac{1 + \beta \delta_0 \alpha_K}{1 + \beta \delta_0 \alpha_K (1 - \ln(\beta) / \ln(\Lambda_K / \Lambda_N))}.$$

Combining the expressions for μ^+ and μ^- from pions (Eq. 13) and from kaons (Eqs. 15 and 16), the muon charge ratio is

$$\begin{aligned} \frac{\mu^+}{\mu^-} &= \left[\frac{f_{\pi^+}}{1 + B_{\pi\mu} \cos(\theta) E_\mu / \epsilon_\pi} + \frac{\frac{1}{2}(1 + \alpha_K \beta \delta_0) A_{K\mu} / A_{\pi\mu}}{1 + B_{K\mu}^+ \cos(\theta) E_\mu / \epsilon_K} \right] \\ &\times \left[\frac{(1 - f_{\pi^+})}{1 + B_{\pi\mu} \cos(\theta) E_\mu / \epsilon_\pi} + \frac{(Z_{NK^-} / Z_{NK}) A_{K\mu} / A_{\pi\mu}}{1 + B_{K\mu} \cos(\theta) E_\mu / \epsilon_K} \right]^{-1}. \quad (17) \end{aligned}$$

For the pion contribution, isospin symmetry allows the pion terms in the numerator and denominator to be expressed in terms of f_π^+ as defined after Eq. 14 above. The kaon contribution does not have the same symmetry. Numerically, however, the differences are at the level of a few per cent, as discussed in the results section.

3. Primary spectrum of nucleons

What is relevant for calculating the inclusive spectrum of leptons in the atmosphere is the spectrum of nucleons per GeV/nucleon. This is because, to a good approximation, the production of pions and kaons occurs at the level of collisions between individual nucleons in the colliding nuclei. To obtain the composition from which the spectrum of nucleons can be derived we use the measurements of CREAM [6, 7], grouping their measurements into the conventional five groups of nuclei, H, He, CNO, Mg-Si and Mn-Fe.

Direct measurements of primary nuclei extend only to ~ 100 TeV total energy. Because we want to calculate spectra of muons and neutrinos up to

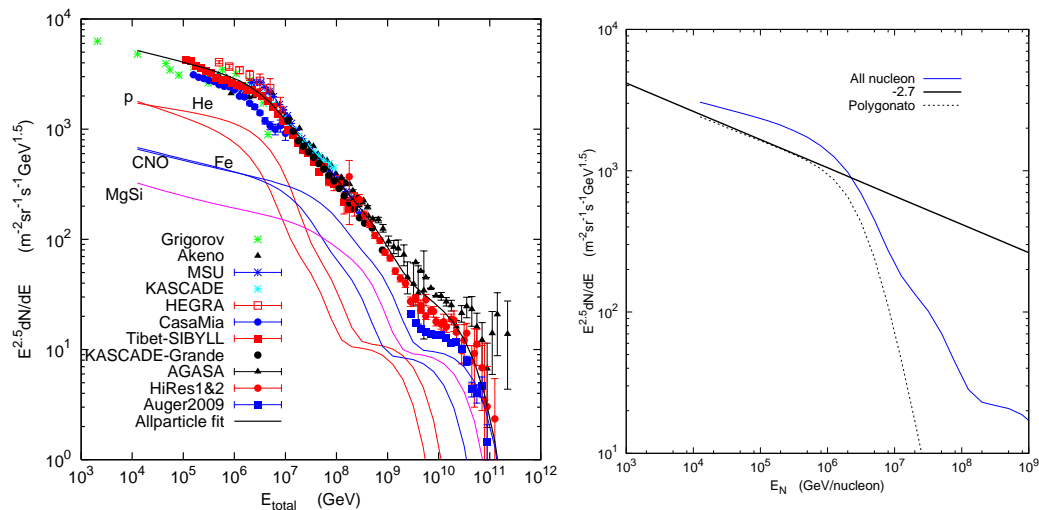


Figure 1: Left: three-population model of the cosmic-ray spectrum from Eq. 21 compared to data [12–22]. The extra-galactic population in this model has a mixed composition. Right: Corresponding fluxes of nucleons compared to an $E^{-2.7}$ differential spectrum of nucleons and to the all nucleon flux implied by the Polygonato model (galactic component only) [25].

a PeV, we need to extrapolate the direct measurements to high energy in a manner that is consistent with measurements of the all-particle spectrum by air shower experiments in the knee region (several PeV) and beyond, as illustrated in the left panel of Fig. 1. To do this we adopt the proposal of Hillas [23] to assume three populations of cosmic rays. The first population can be associated with acceleration by supernova remnants, with the knee signaling the cutoff of this population. The second population is a higher-energy galactic component of unknown origin (“Component B”), while the highest energy population is assumed to be of extra-galactic origin.

Following Peters [24] we assume throughout that the knee and other features of the primary spectrum depend on magnetic rigidity,

$$R = \frac{pc}{Ze}, \quad (18)$$

where Ze is the charge of a nucleus of total energy $E_{\text{tot}} = pc$. The motivation is that both acceleration and propagation in models that involve collisionless diffusion in magnetized plasmas depend only on rigidity. The rigidity

R_c	γ	p	He	CNO	Mg-Si	Fe
γ for Pop. 1	—	1.66	1.58	1.63	1.67	1.63
Population 1: 4 PV	see line 1	7860	3550	2200	1430	2120
Pop. 2: 30 PV	1.4	20	20	13.4	13.4	13.4
Pop. 3 (mixed): 2 EV	1.4	1.7	1.7	1.14	1.14	1.14
" (proton only): 60 EV	1.6	200.	0	0	0	0

Table 1: Cutoffs, integral spectral indices and normalizations constants $a_{i,j}$ for Eq. 21.

determines the gyroradius of a particle in a given magnetic field B according to

$$r_L = R/B. \quad (19)$$

Peters pointed out that if there is a characteristic rigidity, R_c above which a particular acceleration process reaches a limit (for example because the gyroradius is larger than the accelerator), then the feature will show up in total energy first for protons, then for helium and so forth for heavier nuclei according to

$$E_{tot}^c = A \times E_{N,c} = Ze \times R_c. \quad (20)$$

Here E_N is energy per nucleon, A is atomic mass and Ze the nuclear charge. The first evidence for such a Peters cycle associated with the knee of the cosmic-ray spectrum comes from the unfolding analysis of measurements of the ratio of low-energy muons to electrons at the sea level with the KASCADE detector [15].

In what follows we assume that each of the three components (j) contains all five groups of nuclei and cuts off exponentially at a characteristic rigidity $R_{c,j}$. Thus the all-particle spectrum is given by

$$\phi_i(E) = \sum_{j=1}^3 a_{i,j} E^{-\gamma_{i,j}} \times \exp\left[-\frac{E}{Z_i R_{c,j}}\right]. \quad (21)$$

The spectral indices for each group and the normalizations are given explicitly in Table 1. The parameters for Population 1 are from Refs. [6, 7], which we assume can be extrapolated to a rigidity of 4 PV to describe the knee. In Eq. 21 ϕ_i is $dN/d\ln E$ and γ_i is the integral spectral index. The subscript $i = 1, 5$ runs over the standard five groups (p, He, CNO, Mg-Si and Fe), and the all-particle spectrum is the sum of the five.

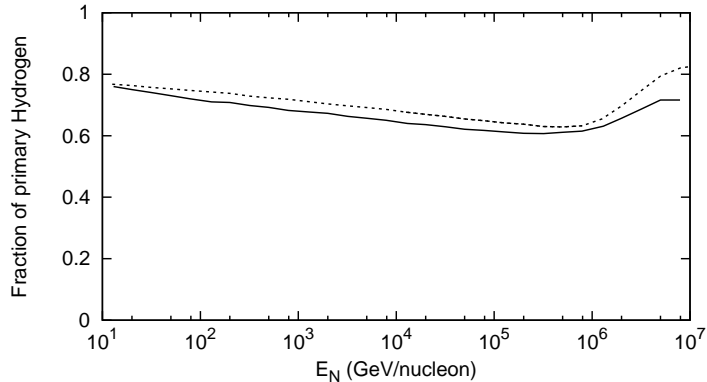


Figure 2: Solid line: charge ratio parameter δ_0 for the model with parameters of Table 1. Dashed line: same for Polygonato model [25].

The composite spectrum corresponding to Eq. 21 and Table 1 is superimposed on a collection of data in the left panel of Fig. 1. No effects of propagation in the galaxy or through the microwave background have been included in this phenomenological model. For the two galactic components, however, a consistent interpretation could be obtained with source spectra $\gamma^* \sim 1.3$ for population 1 and $\gamma^* \sim 1.07$ for population 2 together with an energy dependent diffusion coefficient $D \sim E^\delta$ with $\delta = 0.33$ for both components to give local spectra of $\gamma = \gamma^* + \delta$ of ~ 1.63 and ~ 1.4 respectively. The extragalactic component comes in above the energy region of interest for this paper. We do not discuss it further here except to note that the last line of Table 1 gives the parameters for an extragalactic component of protons only.

The spectrum of nucleons corresponding to Eq. 21 is given by

$$\phi_{i,N}(E_N) = A \times \phi_i(A E_N) \quad (22)$$

for each component and then summing over all five components. The nucleon spectrum is shown in the right panel of Fig. 1.

The energy-dependent charge ratio $\delta_0(E_N)$ needed to calculate the muon charge ratio follows from Eq. 22 and Table 1. To a good approximation, it is given by the fraction of free hydrogen in the spectrum of nucleons, as shown in Fig. 2. The fraction decreases slowly from its low energy value of 0.76 at 10 GeV/nucleon [26] to a minimum of 0.63 at 300 TeV and then increases

somewhat at the knee. Note that, because of the relation among E_{tot} , E_N and R_c in Eq. 20, the steepening at the knee occurs for nuclei at $Z/A \approx \frac{1}{2}$ the energy per nucleon as compared to protons. Hence the free proton fraction rises again at the knee.

Also shown for comparison in Fig. 2 by the broken line is the δ_0 parameter for the rigidity-dependent version of the Polygonato model, which has a common change of slope $\Delta\gamma = 1.9$ at the knee [25]. This gives rise to the sharp cutoff in the spectrum of nucleons for this model in the right panel of Fig. 1. This version of the Polygonato model is meant to describe only the knee of the spectrum and the galactic component of the cosmic radiation. The behavior of the primary spectrum for $E_N > 10^5$ GeV/nucleon does not affect the charge ratio, which is measured only for $E_\mu < 10^4$ GeV. It is therefore possible to consider the difference between the two versions of δ_0 in Fig. 2 as a systematic effect of the primary composition.

4. Comparison with data

We now wish to compare the calculation of Eq. 17 to various sets of data using the energy-dependent primary spectrum of nucleons (Eq. 22) with parameters from Table 1. There are two problems in doing so. First, expressions for the intensity of protons and neutrons from Eqs. 2 and 3 and the subsequent equations are valid under the assumption of a power-law spectrum with an energy independent value of δ_0 . The assumption of a power law with integral spectral index of -1.7 is a reasonable approximation over the range of energies below the knee because it affects both charges in the same way. The proton-neutron difference, however, introduces an explicit energy-dependence into Eq. 17 that must be accounted for. We want to consider the energy range from 10 GeV to PeV over which the composition changes slowly with energy, as shown in Fig. 2. For estimates here we use the approximation $\delta_0(E_N) = \delta_0(10 \times E_\mu)$.

The other problem is that the data are obtained over a large range of zenith angles, and the charge ratio also depends on angle. The first MINOS publication [1] gives μ^+/μ^- as a function of the energy of the muon at the surface. These data are shown in Fig. 3 along with older high energy data from the Park City Mine in Utah [27] and data at lower energy from L3 [28] and CMS [29]. The figure shows three calculations of the muon charge ratio in the vertical direction that follow from Eq. 17. The highest curve assumes a constant composition fixed at its low energy value, $\delta_0 = 0.76$ [26]. The

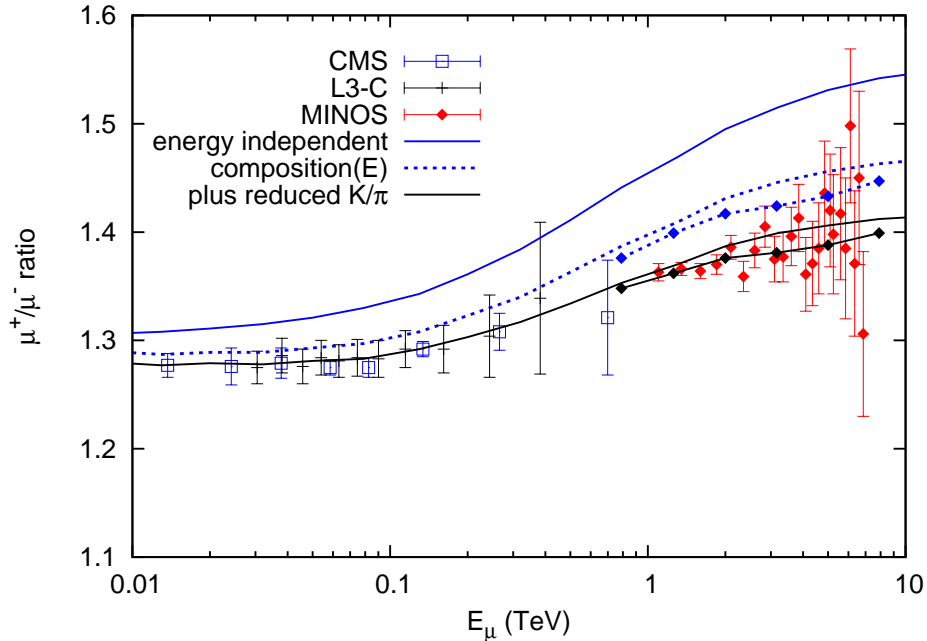


Figure 3: Muon charge ratio compared to data of CMS [29] and L3-C [28] below 1 TeV and to MINOS [1] at higher energy. The L3-C data plotted here are averaged over $0.9 \leq \cos(\theta) \leq 1.0$ for comparison with the calculation for vertical muons. See text for a description of the lines.

middle curve is the result assuming the energy-dependent composition parameter $\delta_0(E_N)$ that corresponds to the parameterization of Table 1 (solid line in Fig. 2), which is still higher than the data. Both the higher lines assume the nominal values of the spectrum weighted moments from Ref. [11]. The lowest curve is obtained by reducing the level of associated production, by changing Z_{pK^+} from its nominal value of 0.0090 to 0.0079

In order to look for the best fit it is necessary first to account for the dependence on zenith angle. The MINOS paper [1] does not give the mean zenith angle for each energy bin. However, because of the flat overburden at the Soudan mine where the MINOS far detector is located, there is a strong correlation between zenith angle and energy at the surface, as illustrated in Fig. 14 of Ref. [1]. Using this relation we estimate the effective zenith angle as a function of energy from $\cos(\theta) \approx 0.9$ at 1 TeV to $\cos(\theta) \approx 0.5$ at 7 TeV.

The points connected by lines in the multi-TeV range show the results of the calculation taking account of the dependence on zenith angle in Eq. 17. The lowest set of points has been adjusted to fit the MINOS data by varying the parameter Z_{pK^+} , which reflects $p \rightarrow K^+$.

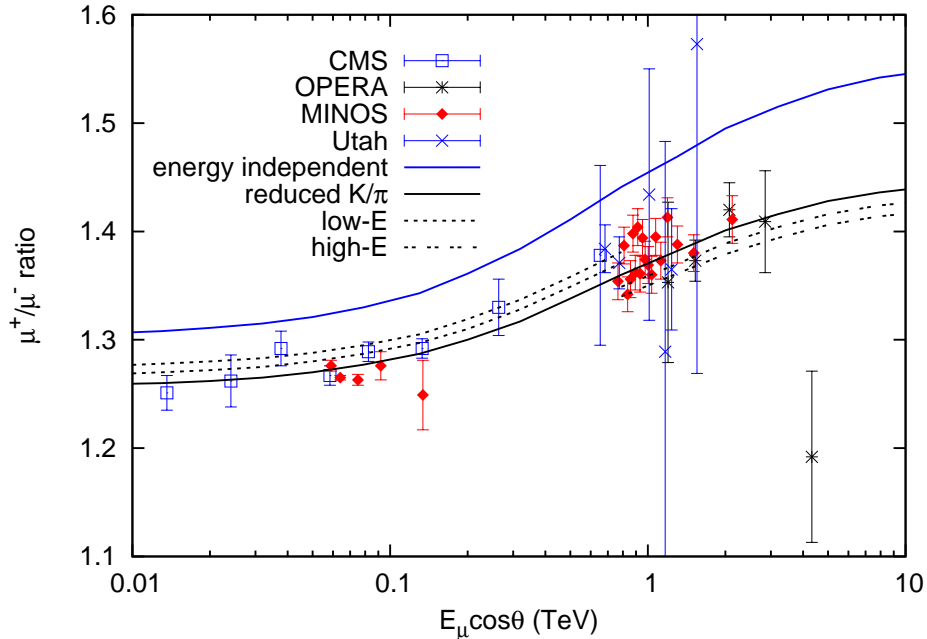


Figure 4: Muon charge ratio compared to data of CMS [29], OPERA [3] and MINOS [2]. Measurements from the near detector of MINOS [30] and from Park City [27].

The dependence of μ^+/μ^- on zenith angle enters Eq. 17 in the form $E_\mu \cos(\theta)$. For this reason the muon charge ratio is often presented as a function of this combination. The data of OPERA are presented only in terms of the product $E_\mu \cos(\theta)$. Because of the complex overburden at Gran Sasso, there is no simple relation between zenith angle and energy. The MINOS data are also presented in this form in Ref. [2], but the mean energy for each value of $E_\mu \cos(\theta)$ is not given. For a primary cosmic-ray composition that has no energy dependence, Eq. 17 depends only on $E_\mu \cos(\theta)$. The effect of the energy-dependence of composition can therefore be assessed by comparing the calculation for various fixed values of δ_0 to the data, which is done in Fig. 4.

The upper curve in Fig. 4 is the same as the corresponding curve in Fig. 3, plotted for a constant composition with $\delta_0 = 0.76$, its value at 10 GeV. The parameter δ_0 decreases from 0.71 at 100 GeV/nucleon to 0.68 at a TeV, and from 0.64 at 10 TeV/nucleon to less than 0.62 at 100 TeV. The full curve through the data in Fig. 4 is evaluated for $\delta_0 = 0.665$. The two broken lines in the low energy region are plotted for 0.71 and 0.69, while those at high energy are for 0.64 and 0.62. A more precise comparison between data and calculation could be made given complete information about the distribution of energy within each bin of zenith angle, but it is clear that the data from the various experiments are reasonably consistent with each other and with the present calculation.

5. Summary

The muon charge ratio is sensitive both to the proton excess in the spectrum of primary cosmic-ray nucleons and to the value of Z_{pK^+} . Using recent data on primary composition, we find a proton excess that decreases steadily from 10 GeV/nucleon to 500 TeV. This portion of the cosmic-ray spectrum produces muons from a few GeV to well over 10 TeV. Assuming associated production (Eq. 6) to be the major uncertainty, a level of associated production in the range $Z_{pK^+} = 0.0079 \pm .0002$ is required to fit the observed charge ratio. For comparison, the nominal value [11] is $Z_{pK^+} = 0.0090$. Keeping the nominal values of all other parameters, the fit here corresponds to a ratio

$$R_{K/\pi} = \frac{Z_{pK^+} + Z_{pK^-}}{Z_{p\pi^+} + Z_{p\pi^-}} = \frac{0.0079 + 0.0028}{0.046 + 0.033} = 0.135. \quad (23)$$

It is interesting that analyses of seasonal variations of TeV muons by MINOS [31] and IceCube [32] also suggest a somewhat lower value of $R_{K\pi}$ than its nominal value of 0.149. On the other hand, the value in Eq. 23 still represents a significant contribution from the K^+ decay channel. If the energy-dependent composition of the Polygonato model is used instead, a good fit is obtained with $Z_{pK^+} = 0.0074$, which reflects the somewhat higher value of δ_0 in the relevant energy range (0.68 as compared to 0.64). The fraction of kaons would be correspondingly lower ($R_{K/\pi} = 0.129$).

In the analysis of MINOS, and also in that of OPERA, the muon charge ratio is written in the form

$$\frac{\mu^+}{\mu^-} = \left[\frac{f_{\pi^+}}{1 + B_{\pi\mu} \cos(\theta) E_\mu / \epsilon_\pi} + \frac{f_{K^+} A_{K\mu} / A_{\pi\mu}}{1 + B_{K\mu} \cos(\theta) E_\mu / \epsilon_K} \right] \times \left[\frac{(1 - f_{\pi^+})}{1 + B_{\pi\mu} \cos(\theta) E_\mu / \epsilon_\pi} + \frac{(1 - f_{K^+}) A_{K\mu} / A_{\pi\mu}}{1 + B_{K\mu} \cos(\theta) E_\mu / \epsilon_K} \right]^{-1} \quad (24)$$

with $A_{K\mu} / A_{\pi\mu} = 0.054$. The more correct Eq. 17 has a different form for the contribution from kaons. In the MINOS analysis the fitted values of the two free parameters are $f_{\pi^+} = 0.55$ and $f_{K^+} = 0.67$. For $E_\mu \sim \text{TeV}$, $\delta_0 \approx 0.64$ for primary energy per nucleon of 10 TeV. Thus $f_{\pi^+} = \frac{1}{2}(1 + \alpha_\pi \beta \delta_0) = 0.55$ in agreement with the MINOS analysis. A precise comparison with the MINOS value for f_{K^+} is not possible for the reasons explained after Eq. 17. However, numerical differences are at the level of a few per cent. For example, $B_{K\mu}^+ \approx 0.95 \times B_{K\mu}$. From Eqs. 15 and 16, the value of $f_{K^+} = \phi_K(E_\mu)^+ / (\phi_K(E_\mu)^+ + \phi_K(E_\mu)^-) \approx 0.69$ in the TeV region for $\delta_0 \approx 0.64$. However, if the expression for the kaon contribution in Eq. 17 is expressed in terms of f_{K^+} there is an additional multiplicative factor less than unity. Thus, although the forms are different, the fits are much the same.

The role of kaons is relatively more important for neutrinos than for muons. Because the muon mass is close to that of the pion, the muon carries most of the energy of the decaying pion. Kaons split the energy almost equally on average between the μ and the ν_μ . The steep spectrum enhances the effect so that kaons are the dominant source of muon neutrinos above a few hundred GeV. Forward production of K^+ is therefore particularly important. The effect is illustrated in Fig. 5, in which the ratio $\nu_\mu / \bar{\nu}_\mu$ is plotted for the same sequence of assumptions as in the plot of the muon charge ratio (Fig. 3). The implications of the muon charge ratio for neutrinos will be the subject of a separate paper.

Acknowledgments: I am grateful to Anne Schukraft and Teresa Montaruli for comments on an early version of this paper. I am grateful for helpful comments from an external reviewer and to Jeffrey de Jong and Simone Biagi for information about MINOS and OPERA. This research is supported in part by the U.S. Department of Energy under DE-FG02-91ER40626.

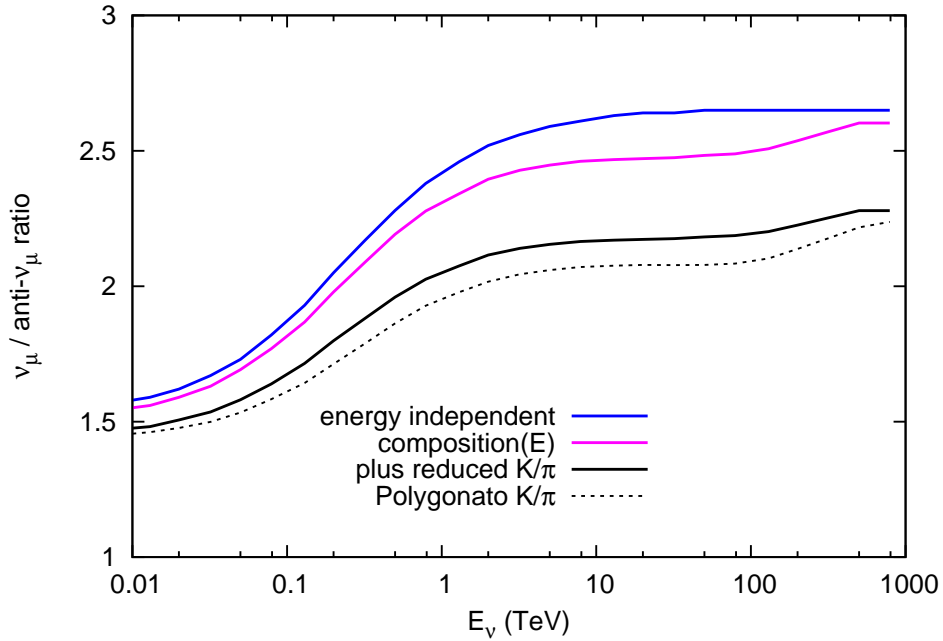


Figure 5: ratio of $\nu_\mu/\bar{\nu}_\mu$ calculated with the same parameters as for the charge ration of muons. The dashed line shows the results with parameters of the Polygonato model [25].

References

- [1] P. Adamson *et al.*, (MINOS Collaboration) Phys. Rev. D **76**, 052003 (2007).
- [2] P.A. Schreiner, J. Reichenbacher, M.C. Goodman, Astropart. Phys. **32**, 61 (2009).
- [3] N. Agafonova *et al.*, (OPERA Collaboration), Eur. Phys. J. C **67**, 25 (2010).
- [4] Paolo Lipari, Astropart. Phys. 1 (1993) 195-227.
- [5] A.D. Panov, *et al.*, Bulletin of the Russian Academy of Sciences: Physics, 73 (2009)564-567.
- [6] H.S. Ahn *et al.*, Ap.J. 714 (2010) L89-L93.

- [7] H.S. Ahn, *et al.*, *Ap.J.* 707 (2009) 593-603.
- [8] O. Adriani *et al.* (PAMELA) *Science* 332 (2011) 69-72.
- [9] W.R. Frazer *et al.*, *Phys. Rev. D* 5 (1972) 1653.
- [10] P. Desiati & T.K. Gaisser, *Phys. Rev. Letters* 105 (2010) 121102.
- [11] *Cosmic Rays and Particle Physics*, T.K. Gaisser, (Cambridge University Press, 1990).
- [12] N.L. Grigorov *et al.*, *Yad. Fiz.* 11 (1970) 1058.
- [13] M. Nagano *et al.* (Akeno), *J. Phys. G* 10 (1984) 1295-1310 and 18 (1992) 423-442.
- [14] Yu. A. Fomin, *et al.* (MSU), *J. Phys. G: Nucl. Part. Phys.* 22 (1996) 1839.
- [15] T. Antoni *et al.*, *Astropart. Phys.* 24 (2005) 1.
- [16] F. Arqueros, *et al.* (HEGRA), *Astronomy & Astrophysics* 359 (2000) 682.
- [17] M.A.K. Glasmacher *et al.* (CASA MIA) *Astropart. Phys.* 10 (1999) 291.
- [18] M. Amenomori, *et al.* (Tibet), *Astrophys. J.* 678 (2008) 1165
- [19] W.D. Apel *et al.* (KASCADE-Grande), *Phys. Rev. Letters* 107 (2011) 171104.
- [20] M. Takeda *et al.* (AGASA) *Astropart. Phys.* 19 (2003) 447.
- [21] R.U. Abbasi *et al.* (HiRes) *Astropart. Phys.* 32 (2009) 53.
- [22] Pierre Auger Collaboration, *Phys. Rev. Letters* 104 (2010) 091101.
- [23] A.M. Hillas, arXiv:astro-ph/0607109.
- [24] B. Peters, *Il Nuovo Cimento* XXII (1961) 800-819.
- [25] Jörg R. Hörandel, *Astropart. Phys.* 19 (2003) 193.

- [26] T.K. Gaisser & Todor Stanev, “Cosmic Rays” in *Reviews of Particle Physics*, K. Nakamura et al., J. Phys. G 37 (2010) 075021.
- [27] G.K. Ashley, J.W. Keuffel & M.O. Larson, Phys. Rev. D **7**, 20 (1975).
- [28] P. Achard et al. (L3 Collaboration) Phys. Lett. B 598 (2004) 15.
- [29] CMS Collaboration, Physics Letters B **692**,83 (2010).
- [30] P. Adamson *et al.*, (MINOS Collaboration) Phys. Rev. D **83**, 032011 (2011).
- [31] MINOS Collaboration (P. Adamson et al.) Phys. Rev. D 81 (2010) 012001.
- [32] IceCube Collaboration (P. Desiati et al.) Proc. 32nd Int. Cosmic Ray Conf. (Beijing, August, 2011).